Theor Appl Climatol (2012) 108:471–477
DOI 10.1007/s00704-011-0541-6

ORIGINAL PAPER

Critical roles of convective momentum transfer in sustaining the multi-scale Madden–Julian oscillation

Fei Liu · Gang Huang · Licheng Feng

Received: 9 August 2011 / Accepted: 14 October 2011 / Published online: 4 November 2011

Abstract To understand the nature and role of multi-scale interaction involved in the Madden–Julian oscillation (MJO), a dynamical model is built based on two essential processes: the convective complex of the MJO modulates the strength and location of synoptic-scale motions, which in turn feed back to the MJO through the convective momentum transfer (CMT). Our results exhibit that: (1) The lower tropospheric easterly CMT coming from the 2-day waves slows down the MJO dramatically; (2) although the lower tropospheric westerly CMT coming from the superclusters can produce the horizontal quadrupole vortex and vertical westerly wind-burst structures of the MJO, it drives the large-scale motions to propagate eastward too fast; (3) the planetary boundary layer provides an instability source for the MJO and pulls the MJO to propagate eastward at a speed of 0~10 ms^{-1}; and (4) the optimal structure of the multi-scale MJO should be: the stronger superclusters/2-day waves prevail in the rear/front part of the MJO and produce lower tropospheric westerly/easterly CMT there. These theoretical results emphasize the role of CMT and encourage further observations in the multi-scale MJO.

F. Liu · G. Huang (✉)
Key Laboratory of Regional Climate-Environment Research for Temperate East Asia, Institute of Atmospheric Physics, Chinese Academy of Sciences,
Beijing 100029, China
e-mail: hg@mail.iap.ac.cn

F. Liu
International Pacific Research Center,
University of Hawaii at Manoa,
Honolulu, HI 96822, USA

L. Feng
National Marine Environmental Forecasting Center,
Beijing 100081, China

1 Introduction

Madden–Julian oscillation (MJO) is a tropical planetary-scale phenomenon with high-frequency eastward-moving super cloud clusters and westward-propagating 2-day waves coupled in its convective complex (Nakazawa 1988). It features an equatorially trapped, planetary-scale, baroclinic circulation with a period centered at 40 to 50 days (Madden and Julian 1971, 1994). Earlier theories on the MJO focused on the direct interaction between large-scale dynamics and convective heating (Lau and Peng 1987; Emanuel 1987; Wang 1988; Hu and Randall 1994; Grabowski and Moncrieff 2004). Recent observations discovered that the MJO is usually coupled with a multi-scale convective complex (Nakazawa 1988; Hendon and Liebmann 1994; Houze et al. 2000; Straub and Kiladis 2003; Haertel and Kiladis 2004; Moncrieff 2004; Slingo et al. 2003; Kikuchi and Wang 2010), where the eastward-propagating superclusters and westward-propagating 2-day waves are enhanced.

These observations motivate studies of understanding roles of multi-scale interaction (MSI) in the MJO using multi-cloud models (Khouider and Majda 2006, 2007; Majda et al. 2007) and multi-scale models (Majda and Biello 2004; Biello and Majda 2005; Majda et al. 2009a). Majda et al. (2009b, 2011) used a dynamical model to study the MSI in the MJO, by treating the wave activity of synoptic motions as a heating source for the MJO. The convective momentum transfer (CMT) process, however, is missed in their works. While the CMT is on an average downscale (damping large scale) in the westerly burst regime of the MJO, the CMT can change from downscale to upscale (Tung and Yanai 2002a, 2002b). The lower tropospheric CMT in the westerly regime can drive the horizontal quadrupole vortex and vertical westerly wind-

burst structures of the MJO (Majda and Biello 2004; Biello and Majda 2005). Actually, these models only consider the one-way interaction, and the instability and phase speed of the MJO cannot be represented by these one-way interaction models. Based on the work of Majda and Biello (2004) and Biello and Majda (2005), Wang et al. (2011) parameterized the CMT of synoptic-scale motions and built a two-way interaction model. Their work emphasized the role of CMT in sustaining the MJO. In their work, however, the location of synoptic-scale motions was specified in the MJO convective complex. In order to study the role of CMT coming from synoptic-scale motions, we improve the MSI model of Wang et al. (2011) to a location-flexible model, in which the location of synoptic-scale motions is no longer specified.

Section 2 summarizes the MSI model of Wang et al. (2011). The role of CMT is illustrated in section 3, and section 4 presents the optimal structure for the multi-scale MJO. This paper ends with a discussion in the last section.

2 The MSI model

2.1 Physical consideration

The model used here is based on the MSI model built by Wang et al. (2011) for studying the role of CMT in the multi-scale MJO, which integrates three essential elements: (a) large-scale equatorial wave dynamics driven by the planetary boundary layer (PBL) frictional convergence instability (Wang 1988; Wang and Li 1994), (b) effects of multi-cloud heating and an instability arising from meso- to synoptic-scale system induced CMT (Majda and Biello 2004; Biello and Majda 2005), and (c) interaction between the planetary-scale and meso- to synoptic-scale systems. The key process of the MSI, the CMT, is usually controlled by the vertical tilt of the synoptic-scale systems. The westward-tilted structure will produce lower tropospheric westerly CMT, while the eastward-tilted structure will produce lower tropospheric easterly CMT (Majda and Biello 2004; Biello and Majda 2005).

In the MJO convective complex, two synoptic-scale motions are observed to be enhanced (Nakazawa 1988): the eastward propagating super cloud clusters and the westward moving 2-day waves. The eastward propagating super cloud clusters have horizontal convective scale of ~1,500 km, time scale of ~10–15 days, and eastward phase speed of 15–20 ms^{-1} (Nakazawa 1988; Wheeler and Kiladis 1999; Wheeler et al. 2000). They involve heavy precipitation and fully developed deep convection and stratiform clouds, and show a westward tilt in the Rossby-gyre region of the active MJO (Moncrieff and Klinker 1997; Houze et al. 2000). The westward-propagating 2-day waves, identified as n=1 westward Inertio-gravity waves (Takayabu 1994; Haertel and Kiladis 2004; Haertel et al. 2008; Liu and Wang 2011; Liu et al. 2011), have zonal convective scale of ~1,000 km, time scale of ~2 days, and westward propagation speed of 10–30 ms^{-1}. They involve the interaction between the congestus cloud heating, the deep convective heating, and the stratiform heating, and show an eastward tilt in the front of the MJO (Kikuchi and Wang 2010).

2.2 Parameterization of the CMT

The westward/eastward tilt of the superclusters/2-day waves in the MJO convective complex produces lower tropospheric westerly/easterly CMT (Majda and Biello 2004; Biello and Majda 2005). Based on the assumptions: (a) synoptic-scale motions have weak temperature gradient (Majda and Klein 2003), (b) synoptic heating involves two vertical modes: deep convective (sin (z)) and stratiform/congestus (sin(−2z)/sin(2z)), and (c) the stratiform/congestus heating lags/leads (with respect to the propagating direction of synoptic-scale motions) the deep convective heating by a spatial phase of ϕ_0. So the CMT that comes from superclusters or 2-day waves can be parameterized as (Majda and Biello 2004; Biello and Majda 2005)

$$F^U = \pm\frac{1}{2}AF(X)^2\alpha(1-\alpha)\sin(\phi_0)V_{er}(P)M(y). \quad (1)$$

The positive/negative sign represents the westerly/easterly CMT coming from the superclusters/2-day waves. A represents the dimensional amplitude. $F(X)$ is the zonal envelope function of synoptic-scale motions, and its structure will be described in the MSI model. α stands for the relative strength of deep convective to the total heating. The strength of the stratiform and congestus heating is assumed to be equal, i.e., (1−α)/2. Then, the amplitude of the CMT is α(1−α)/2, the product of the amplitude of stratiform/congestus and deep convective heating. Keep in mind that in the works of Majda and Biello (2004) and Biello and Majda (2005), α denotes the strength of stratiform heating relative to the direct deep convective heating. The vertical structure $V_{er}(P) = \cos[(P_e - P)/(P_e - P_t)\pi] - \cos[3(P_e - P)/(P_e - P_t)\pi]$ results from the interaction between the stratiform/congestus and deep convective heating. P_e and P_t denote the pressure at the top of the PBL and the free troposphere, respectively. $M(y) = 2H^2 + yHH_y$ with $H = e^{-2y^2}$ denote the meridional structure of planetary- or synoptic-scale waves.

In the following, U, V, and W denote the zonal (X), meridional (y) wind, and vertical pressure (P) velocity, respectively. T and Φ are the temperature and geopotential height, respectively. Use characteristic velocity scale $C_0 = \sqrt{S\Delta p^2/2} \approx 49 ms^{-1}$ (the gravest internal gravity wave

speed, Wang 1988), length scale $L_c = \sqrt{C_0/\beta} \approx 1460km$, time scale $T_c = 1/\sqrt{\beta C_0} = 0.34Day$, and geopotential height scale C_0^2, where $S = (T/\theta)\partial\theta/\partial P = 3 \times 10^{-6}$ $m^2 s^{-2} Pa^{-2}$ (the static stability parameter), $\beta = f_y = 2 \times 10^{-11} m^{-1}$ s^{-1}(where f is the Coriolis parameter). The nondimensional governing equations for the MSI model on the first baroclinic mode becomes (Wang et al. 2011)

$$U_{1t} - yV_1 + \Phi_{1X} = F_1^U, \tag{2}$$

$$yU_1 + \Phi_{1y} = 0, \tag{3}$$

$$\Phi_{1t} + (U_{1X} + V_{1y}) = -\alpha\overline{q}_1, \tag{4}$$

$$\overline{q}_1 = c_2(\nabla^2\Phi_1 - \Phi_{1X}) - c_3(U_{1X} + V_{1y}), \tag{5}$$

For simplicity, we neglect the damping terms in the momentum and thermodynamic equations. $\overline{q}_1$ is the lower tropospheric moisture convergence, which comes from the PBL Ekman pumping and the free tropospheric convergence. The nondimensional coefficients $c_2 = \frac{\sqrt{\beta C_0}}{E}\frac{\Delta p_b}{P_M}(q_b - q_c)\frac{L_q R}{C_0^2 C_p}$ and $c_3 = \frac{\Delta P}{P_M} q_c \frac{L_q R}{C_0^2 C_p}$ denote, respectively, parameters associated with the PBL moisture convergence, and the lower tropospheric moisture convergence. $R = 287\mathrm{J/(kg \cdot K)}$ is the specific gas constant, and $C_p = 1004\mathrm{J/(kg \cdot K)}$is the specific heat at constant pressure. $L_q = 2.5 \times 10^6\mathrm{J/kg}$ is the latent heat of condensation, $E = 3 \times 10^{-5} s^{-1}$ is the Ekman damping coefficient, $p_e = 900\mathrm{hPa}$ is the pressure at the top of the PBL, and $\Delta P_b = P_s - P_e$ is the PBL depth. The others are surface pressure$P_s = 1,000\mathrm{hPa}$, top tropospheric pressure $P_t = 100\mathrm{hPa}$, free troposphere depth$\Delta P = (P_e - P_t)/2$, and mid-tropospheric height $P_M = (P_e + P_t)/2$. $q_b = \frac{1}{\Delta p}\int_{P_e}^{P_s} q(P)\mathrm{d}P$ and $q_c = \frac{1}{\Delta p}\int_{P_m}^{P_e} q(P)\mathrm{d}P$ denote the mean specific humidity in the PBL and the lower troposphere, respectively. The mean state moisture profile $q(P)$ is assumed to decrease upward exponentially from q_s at the surface with an e-fold scale of 2.2 km. The surface specific humidity is a function of sea surface temperature (SST): $q_s = (0.972\mathrm{SST} - 8.92) \times 10^{-3}$(Wang 1988). In this study, SST is taken as a constant value of 28°C at the equator and decays exponentially poleward with an e-fold scale of 15° of latitude.

Assuming that the CMT envelope of synoptic-scale motions is determined by the planetary-scale moisture convergence, $\overline{q}_1$. The zonal ($F(X)^2$) and meridional ($M(y)$) structures of CMT envelope can both be represented by $\overline{q}$, i.e., $F(X)^2 M(y) = \overline{q}_1$ in Eq. 1, because we only separate different scales in the zonal variables while not in the meridional variables. So the first baroclinic CMT can be written as

$$F_1^U = \pm c_1\alpha(1-\alpha)\overline{q}_1, \tag{6}$$

where $c_1 = 4A\sin(\phi_0)/(3\pi C_0\sqrt{\beta C_0})$, is the nondimensional coefficient associated with the CMT (Wang et al. 2011), here $\phi_0 = \pi/4$. The dimensional amplitude of the CMT is taken as $A = 0.1ms^{-2}$, to produce $\alpha(1-\alpha)c_1 = 10$ with α=0.5. Similar amplitude was used in Majda and Biello (2004).

The MJO have a large Kelvin wave component (Wang et al. 1990), and we seek an analytical solution of moist Kelvin waves to study the multi-scale MJO. The solution of the moist Kelvin waves has the structure of

$$(U_1, V_1, \Phi_1, \overline{q}_1) = (U_{10}, V_{10}, \Phi_{10}, \overline{q}_{10})e^{i(kX - \sigma t)}, \tag{7}$$

where σ and k are the frequency and wave number, respectively.

In the work of Wang et al. (2011), the westward-tilted superclusters and eastward-tilted 2-day waves were pre-specified in the rear and front part of the MJO, respectively. The planetary-scale zonal wind was used to parameterize the direction of CMT, for example, in the rear part of the MJO, the westerly CMT coming from the superclusters is denoted by the positive sign of the westerly of the MJO; while in the front part of the MJO, the easterly CMT coming from the 2-day waves is represented by the negative sign of the easterly of the MJO. Here we remove this pre-specified limitation, and discuss the roles of synoptic-scale motions in different parts of the MJO. In Eq. 6, the positive sign represents the lower tropospheric westerly CMT coming from the superclusters while the negative sign represents the lower tropospheric easterly CMT coming from the 2-day waves. So we introduce a phase lag γ, which represents the lag between the CMT envelope coming from the 2-day waves and the MJO convective center. Eq. 6 can be rewritten as

$$F_1^U = -c_1\alpha(1-\alpha)\overline{q}_1 e^{-i\gamma}. \tag{8}$$

In Fig. 1, the dependence of phase relation between the CMT envelope (black dash lines), the planetary-scale moisture convergence (red lines), and the planetary-scale zonal wind (blue lines) is plotted on different phases γ. When γ=0, $F_1^U = -c_1\alpha(1-\alpha)\overline{q}_1$, which means that the CMT in the MJO convective complex are all easterlies coming from the 2-day ways. When γ=π, $F_1^U = -c_1\alpha(1-\alpha)\overline{q}_1$, which means that the CMT in the MJO convective complex is all westerly coming from the superclusters. In the left/right part of the circle, the CMT mainly comes from

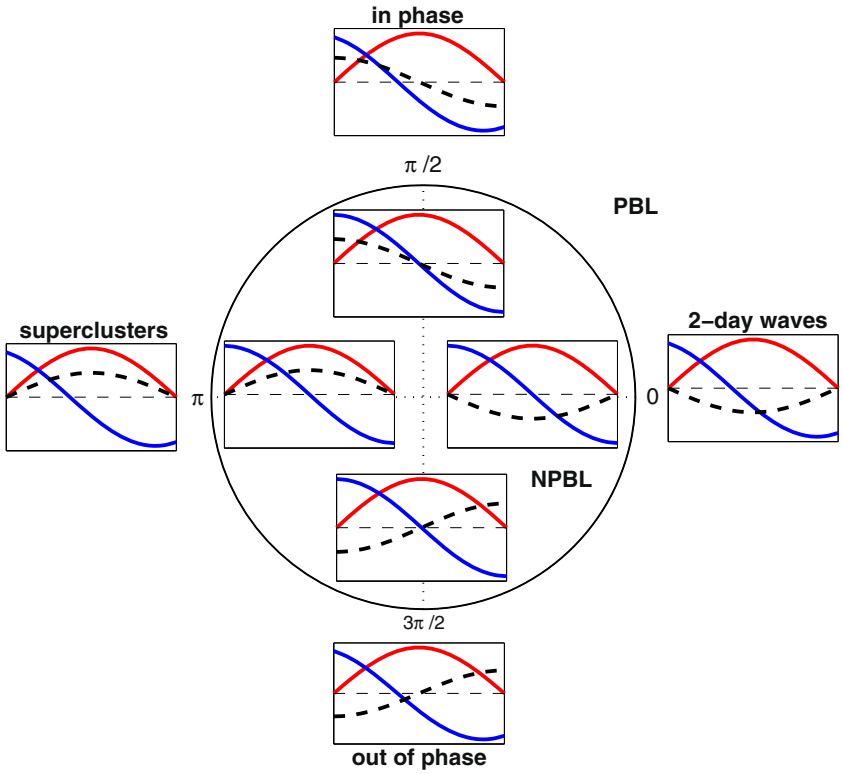

Fig. 1 Dependence of phase relation among the CMT envelope (*black dashed line*), planetary-scale moisture convergence (*red line*), and planetary-scale zonal winds (*blue line*) on different phase γ. The *squares in/out of the circle* represent experiments without/with the frictional planetary boundary layer (*PBL*)

the superclusters/2-day waves in the MJO convective complex. The upper/lower part of the circle denotes that the lower tropospheric CMT is in/out of phase with the lower tropospheric planetary-scale zonal wind. The absolute in-phase relation between the CMT and planetary-scale zonal wind happens at $\gamma=\pi/2$ without the PBL, while it occurs at $\pi/4<\gamma<\pi/2$ when the PBL is included because of the precondition of PBL moisture (Wang 1988).

The simple frequency equation for the MJO can be obtained by setting V and y to zero (Majda et al. 2009b). Substitution of Eqs. 7–8 into Eqs. 2–5 gives

$$\sigma^2+kc_3c_1e^{-i\gamma}(1-\alpha)\sigma-ik^2c_2\alpha\sigma+k^2(c_3\alpha-1) -ik^3c_2c_1e^{-i\gamma}(1-\alpha)=0. \quad (9)$$

The phase speed and growth rate, represented by the real and imaginary part of σ, can be calculated from Eq. 9. Here, we only discuss the planetary-scale MJO of wavenumber one. Experiments show that the results with $k=2$ also have the same features.

3 The roles of CMT

Here we use $\alpha=0.5$, which means that half of total clouds happen at the stratiform/congestus clouds. The role of CMT on the multi-scale MJO can be summarized in Fig. 2 without the PBL and in Fig. 3 with the PBL included.

In Figs. 2 and 3, the contours of phase speed and growth rate are drawn in the *radius*−γ space, where the radius scales the phase speed and growth rate. On each phase γ, phase speed is plotted in log10 scales, which is represented by the radius. Two reference speeds, 10 and 100 ms^{-1} are denoted by dashed lines 10 and 100, respectively. For example, when all CMT comes from 2-day waves, i.e., $\gamma=0$, the system propagates eastward at a speed of about 7 $\mathrm{m\,s}^{-1}$; when all CMT comes from superclusters and $\gamma=\pi$, the system propagates eastward at a speed above 100 ms^{-1} (Fig. 2a). Growth rate is also drawn by the same way, except that its original value is plotted. Two reference growth rates, 0 and 0.2 day^{-1}, are drawn by dashed lines 0 and 0.2, respectively. For example, the growth rate is about 0.02 day^{-1} when $\gamma=\pi/2$ and −0.02 day^{-1} when $\gamma=3\pi/2$.

From Figs. 2 and 3, we can conclude:

1. The CMT coming from 2-day waves/superclusters tends to slow down/fasten the MJO as shown by the right/left part of Fig. 2a. This can be explained by taking $\gamma=0$ for 2-day waves and $\gamma=\pi$ for superclusters. The phase speed of the MJO interacted with 2-day waves (c_{2d}) and superclusters (c_{su}) becomes:

$$c_{2d}=\sigma/k=\sqrt{(1-c_3\alpha)+[c_1c_3\alpha(1-\alpha)/2]^2} -c_1c_3\alpha(1-\alpha)/2, \quad (10a)$$

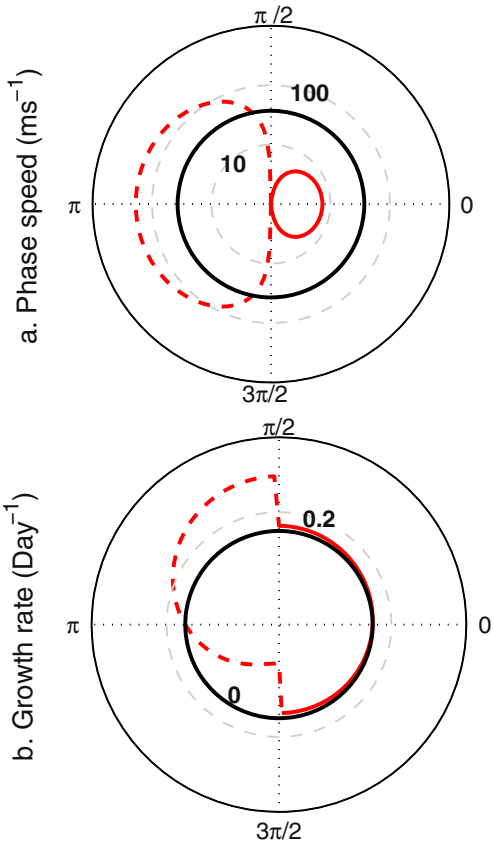

Fig. 2 Dependence of phase speed (**a**) and growth rate (**b**) on different phase γ without the PBL. Phase speed (**a**) and growth rate (**b**) both increase with increasing radius, and the damping domain is located where growth rate is <0. *Red and black lines* represent the experiment with (c_1=20) and without (c_1=0) CMT, respectively. In the *left part of the circles*, the *red lines* are *dashed* to represent the fast mode. Here, α=0.5, and phase speed is plotted by $\log_{10}$

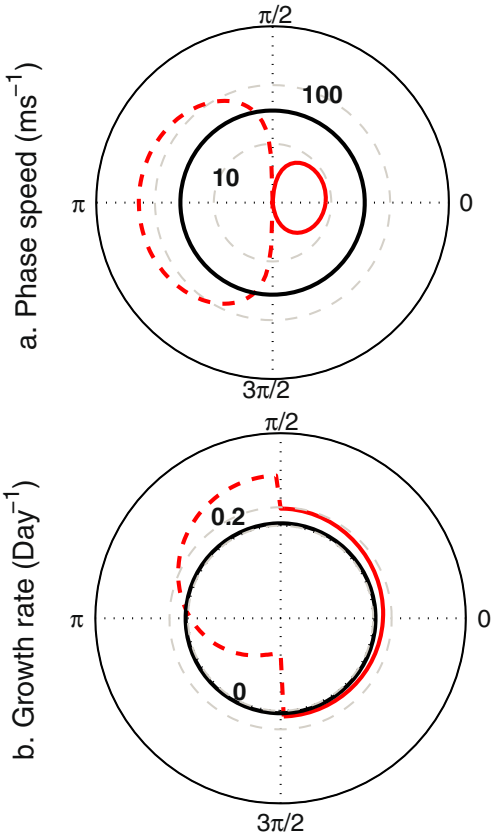

Fig. 3 Same as Fig. 2 except with the frictional PBL included

$$c_{su} = \sigma/k = \sqrt{(1-c_3\alpha) + [c_1c_3\alpha(1-\alpha)/2]^2} + c_1c_3\alpha(1-\alpha)/2. \quad (10b)$$

With increasing CMT, i.e., increasing c_1, c_{2d} decreases to a minimal value of 0 while c_{su} will increase monotonously.

2. Two-day waves try to shrink the phase speed circle into the MJO domain (<10 ms^{-1}) in the right part of Fig. 2a while the superclusters seem to destroy the MJO by driving it into an unrealistic domain of >100 ms^{-1}. It seems that the superclusters cannot drive the MJO alone, although they can produce the horizontal quadrupole vortex and vertical westerly wind-burst structure (Majda and Biello 2004; Biello and Majda 2005).
3. The in/out-of-phase CMT seems to destabilize/decay the MJO as shown by the upper/lower part of Fig. 2b. For example, the frequency at $\gamma=\pi/2$ and $\gamma=3\pi/2$ can be calculated as

$$\sigma(\pi/2) = ikc_3c_1\alpha(1-\alpha)/2 \pm \sqrt{4(1-c_3\alpha) - [kc_3c_1\alpha(1-\alpha)]^2}, \quad (11a)$$

$$\sigma(3\pi/2) = -ikc_3c_1\alpha(1-\alpha)/2 \pm \sqrt{4(1-c_3\alpha) - [kc_3c_1\alpha(1-\alpha)]^2}. \quad (11b)$$

Because the second term is always less than the first term in the right side of Eq. 11a, the growth rate, Im(σ), is always positive for Eq. 11a, but negative for Eq. 11b.

4. Two stationary systems appear at $\gamma=\pi/2$ and $\gamma=3\pi/2$, because when c_1>6.6 with the standard parameters, the last term of Eq. 11 becomes an imaginary number. Under current parameters, c_1 can reach 20 (Majda and Biello 2004; Biello and Majda 2005).
5. It seems that there are two equilibria near $\gamma=\pi/2$ and $\gamma=3\pi/2$ (Fig. 2b). Keep in mind, in this work, we did not show the other solution in the left part, which is the same but in the mirror as the drawn solution in the right part. This solution means that the CMT coming from the superclusters will slow down the westward planetary-scale mode. While in the real atmosphere, the planetary-

scale, westward-propagating systems are seldom observed, and we do not emphasize this solution.

6. Compared with Fig. 2b, Fig. 3b shows that the frictional PBL does provide an instability source for the atmosphere by preconditioning moisture convergence (Wang 1988), especially in the MJO domain (right part of Fig. 3b). This instability even occurs in the original damping domain when $3\pi/2<\gamma<2\pi$ (Fig. 3b).
7. Without the PBL, the in-phase CMT, which is absolutely in phase with the planetary-scale zonal wind, i.e., $\gamma=\pi/2$, produces a stationary system (Fig. 2a). When the PBL is included, this in-phase CMT occurs at $\pi/4<\gamma<\pi/2$, and this model presents an eastward propagating system (Fig. 3a). This means that the Ekman pumping of the PBL, which is under the easterly (Wang 1988), will lead the wave convergence and pull the system forced by the in-phase CMT to propagate eastward (Fig. 3a).

4 The optimal structure for the multi-scale MJO

Based on above results, we obtain the favorable domain for the multi-scale MJO in the $\alpha-\gamma$ space. In Fig. 4, only domain with phase speed between 1 and 9 ms^{-1} is shaded.

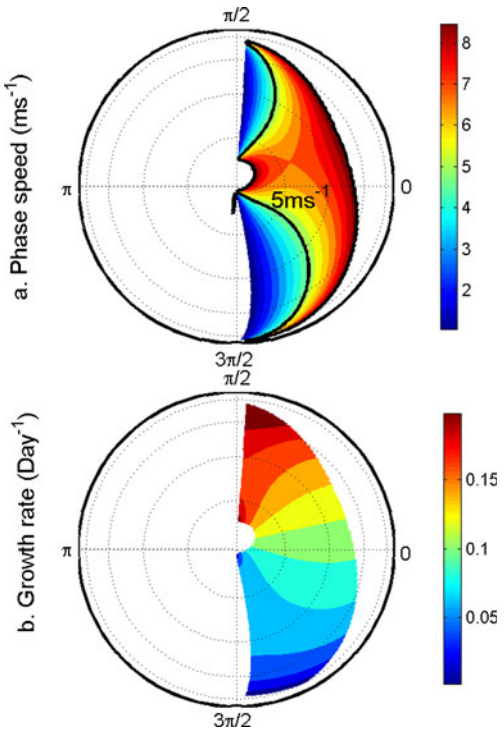

Fig. 4 Phase speed (**a**) and growth rate (**b**) contours in the $\alpha-\gamma$ space. The *solid dark line* in (**a**) denotes constant speed line of 5 ms^{-1}. In the radial direction, from inside to outside, the *dotted circles* represent $\alpha=$ 0.8, 0.6, 0.4, and 0.2, respectively

When the 2-day waves are more active than the superclusters (in the right part of Fig. 4), the unstable system always appears in the MJO domain (0~10 ms^{-1}) with a broad band of cloud structures, $0.4<\alpha<0.8$, especially for $\alpha=0.5$ associated with strong stratiform/congestus clouds. This result is in accord with previous works that strong stratiform clouds are necessary for sustaining the MJO (Schumacher and Houze 2003; Fu and Wang 2009). The most unstable system usually occurs at $\pi/4<\gamma<\pi/2$, where easterly/westerly CMT is located in the front/rear part of the MJO, and is almost in phase with the planetary-scale zonal wind (Fig. 1): the 2-day waves prevail in front part of the MJO convective complex and produce low tropospheric easterly CMT, while the superclusters overwhelm the 2-day waves in the rear part, i.e., the Rossby-gyre region of the MJO (Moncrieff and Klinker 1997), and produce low tropospheric westerly CMT. Such optimal structure is consistent with the multi-scale structure of observed MJO (Moncrieff and Klinker 1997; Kikuchi and Wang 2010). Using this structure, Biello and Majda (2005) obtained the horizontal quadrupole vortex and vertical westerly windburst structures of the MJO, and Wang et al. (2011) also successfully simulated the phase speed and structures of the unstable MJO.

5 Concluding discussion

Based on the dynamical MSI model, we present that the CMT coming from 2-day waves tends to slow down the MJO. In the multi-cloud model (Majda et al. 2007), the popular westward moving inertio-gravity waves coupled in the MJO convective complex may be the key for maintaining the slow eastward propagation of the MJO. Although the CMT coming from the superclusters can explain the horizontal quadrupole vortex and vertical westerly windburst structures of the MJO (Majda and Biello 2004; Biello and Majda 2005), it alone cannot maintain the MJO system because it will increase the speed of the original fast moist Kelvin waves. The PBL still produces an instability source to the atmosphere (Wang 1988) and pulls the MJO to propagate eastward. Usually, the most optimal structure for the multi-scale MJO is: the superclusters, coupled with the deep convection and stratiform clouds, prevail in the rear part of the MJO, while 2-day waves prevail in the front part of the MJO (Fig. 4). This optimal structure is consistent with the observations (Moncrieff and Klinker 1997; Johnson and Lin 1997; Houze et al. 2000; Kikuchi and Wang 2010), and consistent with the structure used in the previous one-way (Biello and Majda 2005) or two-way (Wang et al. 2011) interaction model of the MJO.

The theoretical results emphasize the role of CMT in the multi-scale MJO and encourage high-resolution observa-

tions on these multi-scale structures. The multi-scale parameterization can be improved in current general circulation models to improve their ability of the MJO simulation.

Acknowledgments This work was supported by the National Basic Research Program of China (2011CB309704), Special Scientific Research Project for Public Interest (grant no. GYHY201006021), National Natural Science Foundation of China (grant nos. 40890155, 40775051, U0733002, 40906014, and 40976015), and the Youth Marine Science Foundation of State Oceanic Administration (2010218).

References

Biello JA, Majda AJ (2005) A new multiscale model for the Madden–Julian oscillation. J Atmos Sci 62:1694–1721

Emanuel KA (1987) An air-sea interaction model of intraseasonal oscillations in the Tropics. J Atmos Sci 44:2324–2340

Fu X, Wang B (2009) Critical roles of the stratiform rainfall in sustaining the Madden–Julian oscillation: GCM experiments. J Climate 22:3939–3959

Grabowski WW, Moncrieff MW (2004) Moisture-convection feedback in the Tropics. Q J R Meteorol Soc 130:3081–3104

Haertel PT, Kiladis GN (2004) Dynamics of 2-day equatorial waves. J Atmos Sci 61:2707–2721

Haertel PT, Kiladis GN, Denno A, Rickenbach T (2008) Vertical mode decompositions of 2-day waves and the Madden–Julian oscillation. J Atmos Sci 65:813–833

Hendon HH, Liebmann B (1994) Organization of convection within the Madden–Julian oscillation. J Geophys Res 99:8073–8084

Houze RA Jr, Chen SS, Kingsmill DE, Serra Y, Yuter SE (2000) Convection over the Pacific warm pool in relation to the atmospheric Kelvin–Rossby wave. J Atmos Sci 57:3058–3089

Hu Q, Randall DA (1994) Low-frequency oscillations in radiative–convective systems. J Atmos Sci 51:1089–1099

Johnson RH, Lin X (1997) Episodic trade wind regimes over the western Pacific warm pool. J Atmos Sci 54:2020–2034

Khouider B, Majda AJ (2006) A simple multicloud parameterization for convectively coupled tropical waves. Part I: linear analysis. J Atmos Sci 63:1308–1323

Khouider B, Majda AJ (2007) A simple multicloud parameterization for convectively coupled tropical waves. Part II. Nonlinear simulations. J Atmos Sci 64:381–400

Kikuchi K, Wang B (2010) Spatiotemporal wavelet transform and the multiscale behavior of the Madden–Julian oscillation. J Climate 23:3814–3834

Lau KM, Peng L (1987) Origin of low-frequency (intraseasonal) oscillations in the tropical atmosphere. Part I: basic theory. J Atmos Sci 44:950–972

Liu F, Wang B (2011) A model for the interaction between the 2-day waves and moist Kelvin waves. J Atmos Sci. doi:10.1175/JAS-D-11-0116.1

Liu F, Huang G, Feng L (2011) Why do 2-day waves propagate westward? Theor Appl Climatol. doi:10.1007/s00704-011-0450-8

Madden R, Julian P (1971) Detection of a 40–50 day oscillation in the zonal wind in the tropical Pacific. J Atmos Sci 28:702–708

Madden R, Julian P (1994) Observations of the 40–50-day tropical oscillation—a review. Mon Weather Rev 122:814–837

Majda AJ, Klein R (2003) Systematic multiscale models for the tropics. J Atmos Sci 60:393–408

Majda AJ, Biello JA (2004) A multiscale model for the intraseasonal oscillation. Proc Natl Acad Sci USA 101:4736–4741

Majda AJ, Biello JA, Klein R, Stechmann SN, Khouider B (2007) Madden-Julian oscillation analog and intraseasonal variability in a multicloud model above the equator. Proc Natl Acad Sci USA 104:9919–9924

Majda AJ, Biello JA, Klein R, Stechmann SN (2009a) A simple dynamical model with features of convective momentum transport. J Atmos Sci 66:373–392

Majda AJ, Biello JA, Klein R, Stechmann SN (2009b) The skeleton of tropical intraseasonal oscillation. Proc Natl Acad Sci 106:8417–8422

Majda AJ, Biello JA, Klein R, Stechmann SN (2011) Nonlinear dynamics and regional variations in the MJO skeleton. J Atmos Sci. doi:10.1175/JAS-D-11-053.1

Moncrieff MW (2004) Analytic representation of the large-scale organization of tropical convection. J Atmos Sci 61:1521–1538

Moncrieff MW, Klinker E (1997) Organized convective systems in the tropical western Pacific as a process in general circulation models: a TOGA COARE case study. Q J R Meteorol Soc 123:805–827

Nakazawa T (1988) Tropical super clusters within intraseasonal variations over the western Pacific. J Meteorol Soc Jpn 66:823–836

Schumacher C, Houze RA Jr (2003) Stratiform rain in the tropics as seen by the TRMM precipitation radar. J Climate 16:1739–1756

Slingo JM, Inness P, Neale R, Woolnough S, Yang GY (2003) Scale interactions on diurnal to seasonal timescales and their relevance to model systematic errors. Ann Geophys 46:139–155

Straub KH, Kiladis GN (2003) Interactions between the boreal summer intraseasonal oscillation and higher-frequency tropical wave activity. Mon Wea Rev 131:945–960

Takayabu YN (1994) Large-scale cloud disturbances associated with equatorial waves. Part II: westward propagating inertio-gravity waves. J Meteorol Soc Jpn 72:451–465

Tung WW, Yanai M (2002a) Convective momentum transport observed during the TOGA COARE IOP. Part I: general features. J Atmos Sci 59:1857–1871

Tung WW, Yanai M (2002b) Convective momentum transport observed during the TOGA COARE IOP. Part II: case studies. J Atmos Sci 59:2535–2549

Wang B (1988) Dynamics of tropical low-frequency waves: an analysis of the moist Kelvin wave. J Atmos Sci 45:2051–2065

Wang B, Li T (1994) Convective interaction with boundary layer dynamics in the development of the tropical intraseasonal system. J Atmos Sci 51:1386–1400

Wang B, Li T, Liu F, Rui H (1990) Dynamics of the coupled moist Kelvin–Rossby wave on an equatorial beta-plane. J Atmos Sci 47:397–413

Wang B, Li T, Liu F (2011) A model for scale interaction in the Madden–Julian oscillation. J Atmos Sci. doi:10.1175/2011JAS3660.1

Wheeler M, Kiladis GN (1999) Convectively coupled equatorial waves: analysis of clouds and temperature in the wavenumber-frequency domain. J Atmos Sci 56:374–399

Wheeler M, Kiladis GN, Webster PJ (2000) Large-scale dynamical fields associated with convectively coupled equatorial waves. J Atmos Sci 57:613–640